Heavy ion fusion science research for high energy density physics and fusion applications*

B G Logan[1], J J Barnard[2], F M Bieniosek[1], R H Cohen[2], J E Coleman[1], R C Davidson[3], P C Efthimion[3], A Friedman[2], E P Gilson[3], W G Greenway[1], L Grisham[3], D P Grote[2], E Henestroza[1], D H H Hoffmann[4], I D Kaganovich[3], M Kireeff Covo[2], J W Kwan[1], K N LaFortune[2], E P Lee[1], M Leitner[1], S M Lund[2], A W Molvik[2], P Ni[1],G E Penn[1], L J Perkins[2], H Qin[3], P K Roy[1], A B Sefkow[3], P A Seidl[1], W Sharp[2] E A Startsev[3], D Varentsov[4], J-L Vay[1], W L Waldron[1], J S Wurtele[1], D Welch[4], G. A. Westenskow[1] and S S Yu[1]
[1] Lawrence Berkeley National Laboratory, Berkeley, CA 94720, USA
[2] Lawrence Livermore National Laboratory, Livermore, CA, 94551, USA
[3] Princeton Plasma Physics Laboratory, Princeton, NJ 08543, USA
[4] Gesellschaft fur Schwerionenforschung mbH, Darmstadt, Germany
[5] Voss Scientific, Albuquerque, NM, USA
Corresponding Author's E-mail: bglogan@lbl.gov

Abstract
During the past two years, the U.S. heavy ion fusion science program has made significant experimental and theoretical progress in simultaneous transverse and longitudinal beam compression, ion-beam-driven warm dense matter targets, high brightness beam transport, advanced theory and numerical simulations, and heavy ion target designs for fusion. First experiments combining radial and longitudinal compression of intense ion beams propagating through background plasma resulted in on-axis beam densities increased by 700X at the focal plane. With further improvements planned in 2007, these results will enable initial ion beam target experiments in warm dense matter to begin next year at LBNL. We are assessing how these new techniques apply to low-cost modular fusion drivers and higher-gain direct-drive targets for inertial fusion energy.

1. Introduction

A coordinated heavy ion fusion science program by the Lawrence Berkeley National Laboratory, Lawrence Livermore National Laboratory, and Princeton Plasma Physics Laboratory (the Heavy-Ion Fusion Science Virtual National Laboratory), together with collaborators at Voss Scientific and GSI, pursues research on compressing heavy ion beams towards the high intensities required for creating high energy density matter and fusion energy. Previously, experiments in the Neutralized Drift Compression Experiment (NDCX) and simulations showed increases in focused beam intensities first by transverse focusing [1, 2] and then by longitudinal compression (>50 X) with an induction buncher that imparts increasing ion velocities from the head to the tail of a selected 150 ns slice of beam [3, 4]. Section 2 describes new work on combined radial and longitudinal compression of intense beams within neutralizing plasma. In Section 3 we describe the first joint U.S.-German warm dense matter experiments with porous targets using intense beams from the SIS 18 storage ring at GSI [5], together with plans for initial warm dense matter targets at LBNL next year. Progress in e-cloud research is presented in Section 4, advances in theory and simulations in Section 5, applications to heavy ion fusion in Section 6, and conclusions in Section 7.

2. Combined transverse and longitudinal compression of beams within neutralizing plasma

Recent experiments in NDCX have combined neutralized drift compression with a new final focusing solenoid (FFS) and a new target chamber (Figure 1). The FFS was installed with a new beam target chamber, and the plasma density was measured before installing on the NDCX beam line. Two Filtered Cathodic Arc Plasma Sources (FCAPS) streamed aluminum metal plasma upstream toward the exit of the FFS, and a Langmuir probe was driven from the upstream end of the FFS toward the focal plane of the magnet, 18.27 cm downstream of the midplane of the FFS.

* This research was performed under the auspices of the U.S. Department of Energy by the University of California, Lawrence Berkeley and Lawrence Livermore National Laboratories under Contract Numbers DE-AC02-05CH11231 and W-7405-Eng-48, and by the Princeton Plasma Physics Laboratory under Contract Number DE-AC02-76CH03073.

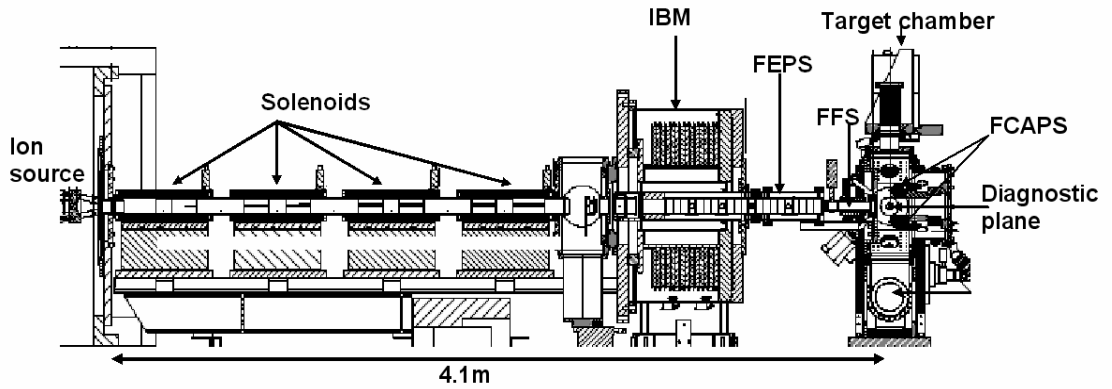

Figure 1: Elevation view of the NDCX. Left to right: 315 keV, 25 mA K^+ ion source, solenoid transport section, induction bunching module (IBM) which imparts the velocity ramp that starts the drift compression of a 150 ns slice of the injected beam, ferroelectric plasma source (FEPS) which neutralizes the longitudinal drift compression region, 5T final focus solenoid (FFS), and new target chamber containing diagnostics at the target plane and two filtered cathodic arc plasma sources (FCAPS).

Theory and simulations of this combined radial and longitudinal compression experiment (see section 5) indicate that achieving maximal beam intensity requires neutralizing plasma densities significantly greater than local beam densities at all points along the drift compression and final focus to target. Figure 2 shows the plasma density distribution as measured with a Langmuir probe on axis between the FFS and the target plane, using LSP particle-in-cell code simulations to estimate the plasma velocity profile needed to infer the local density.

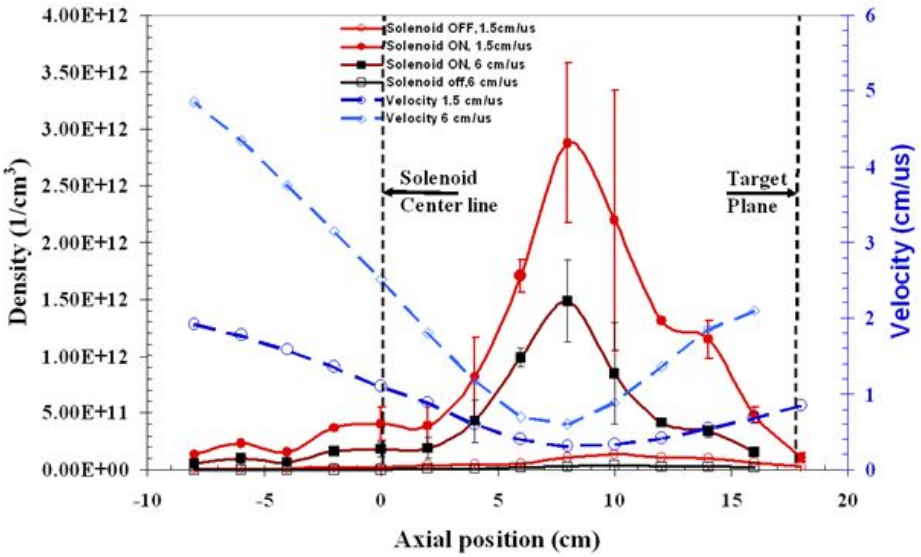

Figure 2: Axial plasma density distributions with and without FFS magnetic field for two initialized FCAPS plasma velocities. The blue dotted lines represent calculated velocities from 2-D LSP simulations initialized with a mean initial velocity of 1.5 cm/μs and 6 cm/μs. The error bars represent the standard deviation of two repeated measurements at each location.

Both measurements and simulations of the neutralizing plasma show that plasma can be guided into the solenoid interior by the magnetic fringe field, close to the axis where the beam propagates, and that the FCAPS plasma density peaks between the FFS magnet exit and the target focal plane. Upstream in the beginning of the drift compression region (a meter to the left in Figure 2), where the incoming beam density is approximately 3.7 x 10^8 cm-3, the beam is well neutralized within the 85 cm long FEPS

plasma of 10^{11} cm^{-3} density. LSP simulations suggest that the actual plasma density distribution has a significant impact on the focal spot. Simulations of the compressing beam along with the assumption of the plasma density much exceeding the beam density throughout the neutralization section predict a radial FWHM of 1 mm. Simulations using plasma density distributions similar to those in Fig. 2 predict a radial FWHM in the range 2-3 mm, depending on the plasma temperature (Section 5).

The target focal plane beam diagnostics were a multiple-pinhole Faraday cup, and a scintillator (the light emission of which was detected using a gated CCD camera). Figure 3 shows the beam profile with and without the FFS energized. FWHM's of 2 mm and 3 mm were measured when the FFS field was 5T and 0 T, respectively. The peak intensity corresponds to a beam density ≈ 2.6 x 10^{11} cm^{-3}, about 700 times the upstream beam density before compression. Figure 2 shows that the plasma density a few centimeters from the target plane, where the beam density increases strongly due to both radial and longitudinal compression, may not be sufficient for complete neutralization of the ion beam. Thus, near-term plans are to repeat the experiment with increased plasma density. Additional improvements planned for this year include new ion sources, increasing the FFS to 8 T, and adding a new induction bunching module (IBM) capable of compressing twice as much ion beam charge from the injector. With these improvements, first warm dense matter target experiments can begin next year. In addition to enabling these experiments, neutralized beam compression and focusing makes possible new high-gain direct drive targets with low range ions for heavy ion fusion (Section 6).

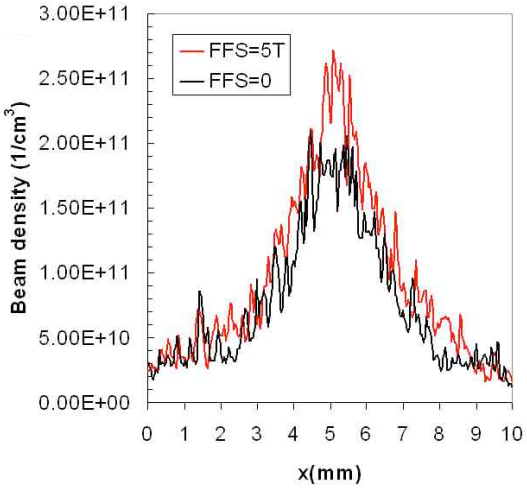

Figure 3: Beam density profiles at the target focal plane with the final focus solenoid on (FFS=5T) and off (FFS=0). The corresponding focal spot FWHM = 2 mm with FFS=5T and 3 mm with FFS=0

3. Warm dense matter experiments: joint experiments at GSI and plans for NDCX

During the past few years, significant progress has been achieved in experimental investigation of heavy-ion-beam-generated warm dense matter (WDM) [6, 7]. The main goals of the joint HIFS-VNL and GSI WDM experiments performed at the HHT area of GSI were commissioning of recently developed diagnostic instruments, methods and testing of different beam-target configurations for EOS studies; optimization of transport, focusing and diagnostics of intense heavy ion beams; obtaining new data on thermophysical properties and hydrodynamic response of various materials in HED states near boiling curve, two-phase liquid-gas and the critical point regions.

Electron-cooled beams ($2.5 \cdot 10^9$ $238U^{73+}$ ions at 350 MeV/u) from the SIS 18 storage ring are compressed to 110 ns (FWHM) and focused at the target down to 150 µm diameter. The beam intensity and the pulse shape have been measured by current transformers installed in front of the target chamber whereas the upper limit for the focal spot size has been determined by recording beam-induced emission of argon gas at ionic spectral lines [8]. In the currently employed plane-HIHEX beam-target configuration, solid or porous sample foils are placed along an elliptically shaped ion beam, at the origin. On either side of the foil, two sapphire plates are located at variable distances parallel to the foil surface, limiting the target expansion and defining the final volume.

Measurements from experiments with porous samples carried out in close GSI-LBNL collaboration are shown in Figure 4. A motorized achromatic 1:1 imaging system built out of two off-axis parabolic

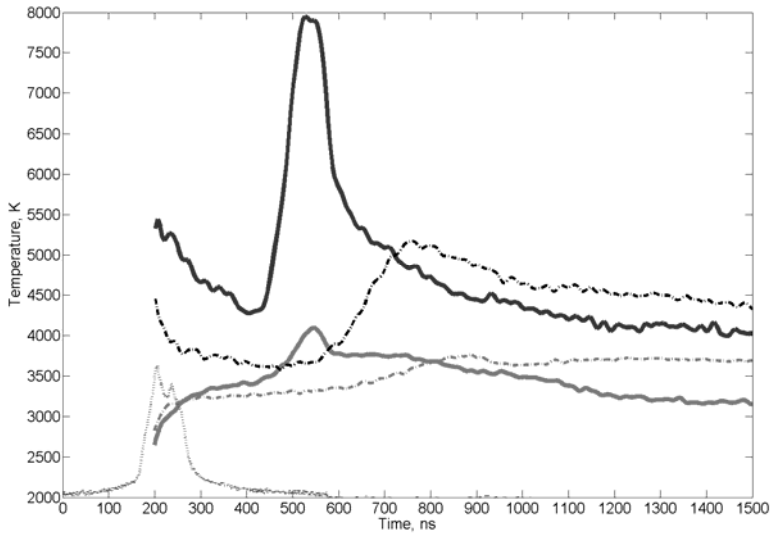

Figure 4: Pyrometer record comparing solid (solid lines) and porous (dashed lines) gold foils. Porous samples are 35% of solid density. Lower solid grey line- brightness temperatures at 900 nm, fitted [9], lower left: dotted line-temporal profile of heating beam in arbitrary units. In the graph, the first peaks are due to heating with beam followed by the decrease in temperature due cooling expansion. Second peaks are caused by impact of the expanded matter against sapphire windows.

mirrors collect light emitted by the beam-heated target and transmits it to a fast radiation pyrometer via 400 micron diameter quartz fiber lines. Using this advanced light collection system and a fast 12-channel pyrometer, the color temperatures in the range 1000 K -16000 K during direct ion-beam heating of tungsten targets have been recorded [9]. The effect of pore size on behavior of porous and solid-density gold and copper targets was studied using existing diagnostics, for example, by measuring the target temperature as a function of pore size and comparing with model predictions of the physics of porous targets. The analysis of experimental results and hydrodynamic simulations are in progress.

Plans for NDCX: A prototype target chamber with multiple diagnostic access ports, a target manipulator and plasma injection has been installed on NDCX (Figure 1).Plans are to measure the temperature and expansion rates of partially-vaporized thin metal foils, e.g., gold or aluminum, to compare with two-phase equations of state models. Incident beam intensity profiles on the target surface will be measured both with a scintillator and light emission of thin gas layers near a hole plate at the target plane. After the ion beam passes through and heats the target foil, it may exit through a hole in the substrate into beam diagnostics such as the beam energy analyzer. A fiber-coupled multi-channel fast optical pyrometer with sub-ns response and temperature sensitivity as low as 1000 C is being developed. Position resolution will be 400 micron or less, depending on the diameter of the coupling fiber. The light collection optics will use a pair of parabolic mirrors and a fiber bundle that carries out thermal light for the pyrometer, as well as light for other optical diagnostics such as the VISAR. Other diagnostics being installed on the NDCX target chamber (Figure 1) include: beam energy analyzer, VISAR system, streak camera, and fast-gated CCD cameras.

4. Progress in e-cloud research

Experiments were performed to study the matching and transport of a space-charge dominated ion beam in the solenoid transport channel shown in Figure 1, including the effects of gas and electrons on the beam. These experiments provide a basis for comparison of solenoid transport with magnetic quadrupole transport in accelerators, for application to warm-dense matter and heavy-ion fusion [10]. The beam energy and current was the same as indicated in Section 2. Solenoid mid-planes are separated by 60 cm. Beam diagnostics are provided in an end tank. The beam at the exit of the diode was also characterized in detail with identical diagnostics.

An e-cloud diagnostics set was installed and commissioned in 2006. Long electrodes in the gaps were placed between magnets (Figure 5), and intercept magnetic flux that expands between magnets and passes through the outer half of the beam radius in the center of solenoids. These “gap electrodes”

are biased positively, in the clearing mode, to remove electrons. Short electrodes are provided in the center of each solenoid; these "solenoid electrodes" are biased negatively, in the clearing mode, to expel electrons from the solenoids. The biases can be reversed for a trapping mode: negatively-biased gap electrodes emit electrons due to ion or photon impact and repel trapped electrons, and positively-biased solenoid electrodes trap electrons in the center of each solenoid magnet. The trapping mode forms a Penning trap with magnetic radial confinement and electrostatic axial confinement of electrons.

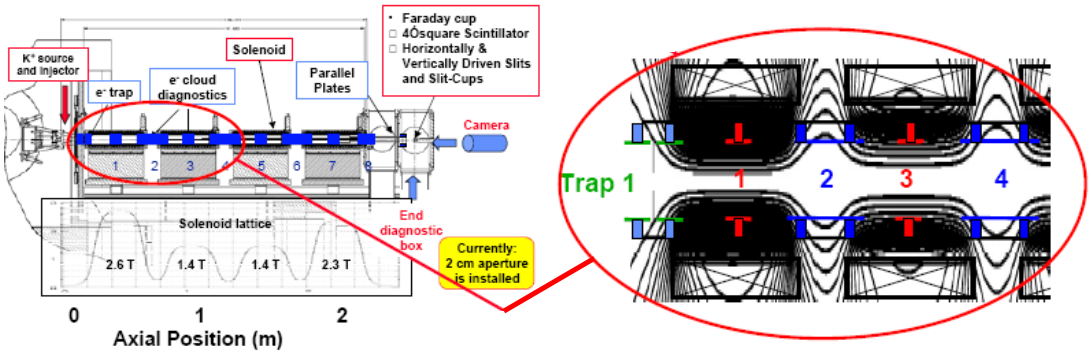

Figure 5: Four solenoid magnets (S1-S4) assembled on the solenoid transport section of the NDCX. The e-cloud diagnostics are shown in blue, labeled with their numbers. The peak magnetic fields are listed for each magnet for the operating beam envelope. The insert shows how the longer gap electrodes intercept magnetic flux that expands outwards between magnets.

Figure 6 shows images of the transverse beam structure taken about 5 μs into a 10 μs beam pulse with a 10-ns gate, show a clear difference between the clearing and trapping bias patterns. The co-ordinate space image for the clearing pattern shows a roughly circular 6.3-cm beam spot, with the density varying by about 25 % across the top plus a small 50% density depression at the center. The transverse phase space for this case shows a beam emittance of 20.9 mm-mrad and a convergence angle of -7.5 mrad. In contrast, a bias set to trap electrons has a larger spot size, a very irregular density profile, and an emittance that is five times larger than is found for the other bias pattern. The case with unbiased electrodes gave intermediate results, closer to the clearing than to the trapping case.

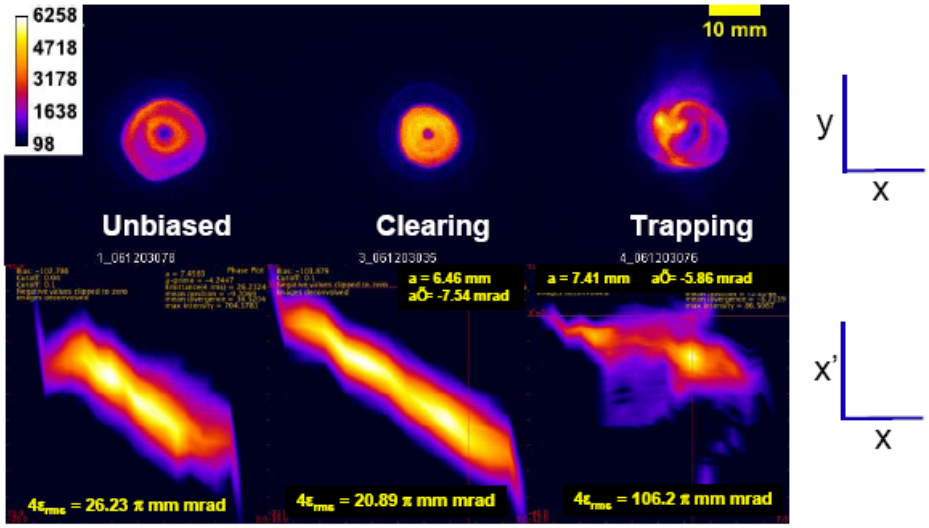

Figure 6: Transverse X-Y coordinate space and X-X' phase space images of the four-solenoid NDCX with internal electrodes unbiased, biased in clearing mode and in trapping mode. Benefits of the clearing mode are evident in lower emittance and lower distortion phase-space in X-X'.

Simulations of clearing and trapping cases provide reasonable agreement with the clearing case, but show little difference in the trapping case. This is possibly due to beam halo that scrapes the electrodes, producing electron and gas emission from the surfaces. Emission currents are measured from negatively biased electrodes consistent with this hypothesis. Without a mechanism to generate the observed gap-electrode current in the trapping case, simulations will not be able to reproduce the trapped electron density or its effects on the beam emittance. When electrons are minimized in either solenoids or magnetic quadrupoles, we find that the measured beam envelope agrees well with simulations [11, 12]. This suggests that we have a reasonable understanding of beam currents transport limits, in the absence of electron effects. Plans for future e-cloud research include exploring current limits that may be imposed by beam halos and associated electron effects over longer transport lengths, and finding methods of mitigating such halos.

5. Advances in theory and integrated simulations

Theory and Modeling: Considerable theoretical progress has been made since the 2005 IFSA meeting [13] in advanced analytical and numerical studies of intense ion beams and their interaction with background plasma. These studies have included: (a) development and application of optimized analytical and particle-in-cell simulation models for intense ion beam charge and current neutralization in solenoidal and dipole magnetic field configurations [14. 15]; (b) detailed theoretical investigations of the dynamic stabilization of the two-stream instability during longitudinal compression of intense charged particle beam propagation through background plasma [16, 17]; (c) development and application of advanced kinetic and macroscopic warm-fluid models to describe longitudinal drift compression and pulse shaping in intense heavy ion beams [18]; ((d) analytical investigations of the multi-species two-stream and electromagnetic Weibel instabilities for intense beam propagation through background neutralizing plasma, and determination of conditions to minimize deleterious effects of the instabilities [19]; (e) development of improved analytical and advanced nonlinear perturbative simulation models using the BEST code, including detailed 3D investigations of collective effects and the Harris and Weibel instabilities in anisotropic ion beams, and the effects of finite-length charge bunches [20 – 23]; (f) development of criteria to minimize halo particle production during the transverse compression of intense charged particle beams, including benchmarking of criteria with WARP simulations [24]; (g) continued improvement and optimization of ionization cross-section models for ion–atom interactions for a wide range of ion and atomic species [25, 26]; (h) development of optimized input distribution functions for advanced particle-in-cell simulations of charged particle beams at high space-charge intensity [27]; (i) advanced LSP numerical simulation studies aimed at optimizing the simultaneous longitudinal and transverse focusing of intense ion beam pulses for warm dense matter applications [28] and the extreme compression of intense heavy ion beam pulses using neutralized drift compression [29, 30]; (j) advanced plasma flow simulations aimed at optimizing cathodic-arc and ferroelectric plasma source performance for neutralized compression experiments [31]; and (k) non-invariance of the range of space and time scales under a Lorentz transformation has been applied to gain an order of magnitude speedup for the calculation of the interaction of relativistic beams with plasma and/or electron clouds [32].

Integrated simulations: 2-D (*r,z*) simulations [33] were carried out using the LSP code to explore the limits to the current density achievable at the simultaneous focal plane with the NDCX experiment (see Figure 1). A 327.4 keV, 21.5 mA K^+ beam with a 1.43 cm radius was initialized with a 0.3 eV transverse and longitudinal temperature (0.126 mm-mrad rms normalized emittance). The beam was injected into the NDCX chamber (3.8 cm radius) just upstream of the 3 cm-wide acceleration gap with an initial pulse length of 0.7 μs. Figure 7 illustrates a design schematic of the NDCX as modeled in the simulations, from the induction bunching module IBM (see Figure 1) to the focal plane.

The IBM imposes approximately a 10% velocity tilt (defined as $\delta v_z/v_z$) to the beam, which then drifts 15 cm through a region containing the electrostatic trap and permanent magnetic dipole that serve to confine the plasma in the drift region. The plasma from the 85 cm-long ferroelectric source (n_{pdrift} = $5x10^{10}$ cm-3, T_{pdrift} = 3 eV) was modeled between the magnetic dipole and a gate valve gap.

An 80.5 kG, 9 cm-long final-focus solenoid filled with plasma was modeled (with fringe-fields) near the end of the drift region in order to ensure that the ion beam undergoes transverse focusing to a minimum spot size coincident with the longitudinal focal plane at z = 429 cm, about 15 cm downstream of the exit of the final-focus solenoid. In this simulation, plasma is assumed to be everywhere to show

the best possible focus, so actual experiments as described in Section 2 are expected to have larger focal spots; simulations involving realistic plasma flow profiles in the configuration shown in Figure 1 have predicted large focal spots by a factor of roughly two, indicating the need to increase the neutralizing plasma density in future experiments, especially near the target.

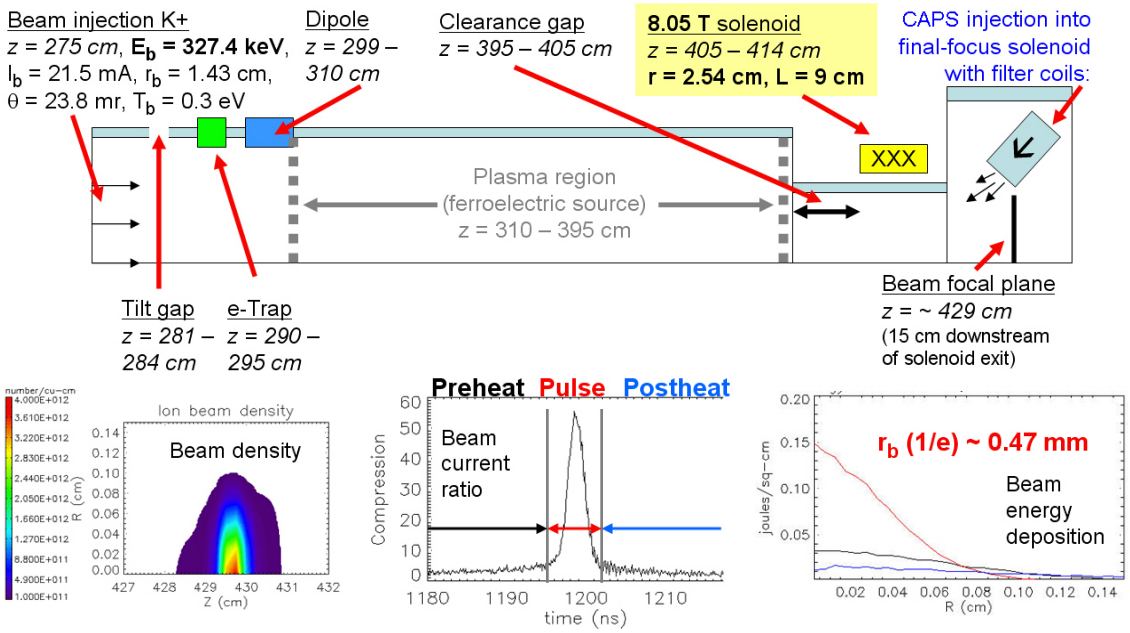

Figure 7: (Top) The simulation model includes the acceleration gap, electrostatic electron trap, permanent magnetic dipole, FEPS, clearance gap, final-focus solenoid, and FCAPS. (Bottom) Beam compression simulation results. The peak beam density (left) reached 4×10^{12} cm^{-3}, the longitudinal current compression ratio was approximately 55X (middle), and the simultaneous radial spot size (1/e) was 0.47 mm (0.9 mm FWHM) with a peak on-axis cumulative energy deposition of 0.15 J cm^{-2} (right). The middle and right plots are color coded to show degree of pre-heat (200 ns total) on the target expected in this configuration.

6. Applications to heavy ion fusion.

The success of strong transverse and longitudinal beam compression in neutralizing plasma, as described in Sections 1 and 5, enables the application of heavy ion beams to direct drive in the ablative rocket regime. Previous work [34] considered low range ion clusters operating as momentum drivers. Here, requirements for high rocket efficiency and low adiabat implosions dictate ion ranges that are a fraction (~0.25) of the initial ablator thickness. Without plasma neutralization, the beam space charge would prevent adequate focusing of the modest-energy ion beams required. Such ions can couple energy into thick fuel capsule ablators at the peak in rocket efficiency, as efficiently as do x-rays in hohlraums, but without the conversion loss of beam energy into x-rays. High ablation velocities with heavy ion direct drive can mitigate hydrodynamic instabilities analogous to x-ray drive but with higher overall beam-to-compressed fuel coupling efficiency.

A simple analytic implosion model with a heavy-ion dE/dx deposition model, together with hydrodynamic implosion calculations using both LASNEX and HYDRA [35], have been used to explore characteristic beam requirements for heavy ion direct drive in the ablative regime, for small 1 MJ drive DT targets as well as for larger tritium-lean (> 90% DD) targets needing 5 MJ drive energy. Ion beams can couple 100 % of their incident energy into hydrogen or DT ablators (most electrons per unit mass) which also have the lowest specific ionization energy $<< u^2_{ex}/2$. However, ion beams can also suffer greater parasitic energy loss when passing through ablation corona plasmas compared to laser or x-ray drive photons, despite the dE/dx Bragg peak near the end of the ion range. Increasing ion energy during the drive pulse (synergistic with velocity ramps used to drift compress the neutralized beams) can reduce the parasitic beam losses on ablated plasma.

Low adiabat implosions are found possible with an initial ion beam range selected to be 25 % of the initial ablator ρr. Overall beam-to-fuel coupling efficiencies >15% are found for small targets driven by 1 MJ of 50 MeV Argon ion beams. This is 4 to 8 times better coupling than that of any hohlraum target, and twice that of any laser direct-drive target, despite major parasitic beam losses (which can be further reduced by optimizing parameters in planned future work. Shock timing control with direct ion drive is sufficient for low adiabat implosions with $\alpha<1.5$ enabling gains ~ 60 at 1MJ (adequate for accelerators of >15 % efficiency), with higher gains possible with more fuel mass. In another example, use of a late ion-driven shock for two-step implosion and ignition shows benefits similar to those of fast ignition; in particular, in 1-D we have obtained ~200 MJ yield at 1.3 MJ (1 MJ for fuel compression and 0.3 MJ for the final shock. Ways to further mitigate ion beam loss on ablation plasma, implosion symmetry requirements for two-sided (polar) direct drive, are planned.

These advances enable T-lean implosions [36- 37] with larger fuel masses sufficient to capture most neutron energy for low cost direct plasma MHD direct conversion [38], as well as to self-breed sufficient tritium from D(d,p)T side reactions to avoid the need for any T breeding in external blankets. By varying the size (ρr) of the DT core for a fixed total ρr=13.5 g/cm^2, *in-situ* T self-breeding ratios greater than unity are possible with reasonable total fusion yields around 500 MJ (see Figure 8).

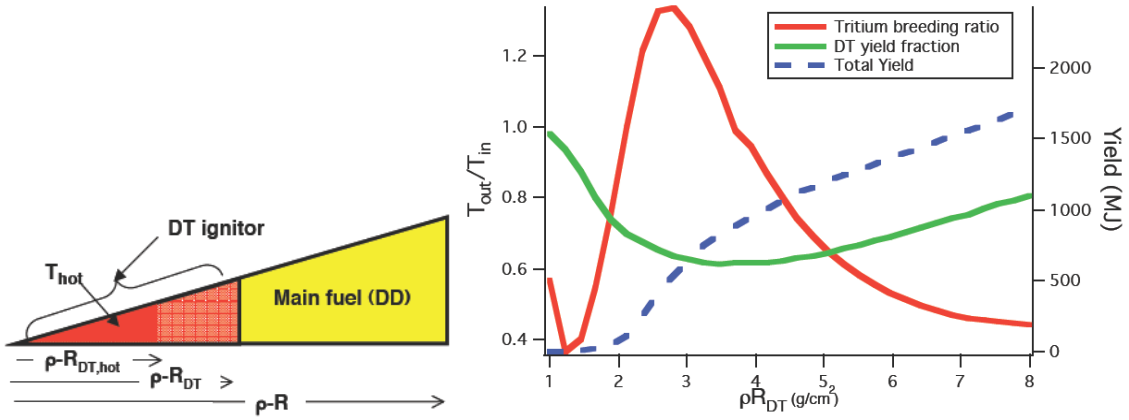

Figure 8: Tritium breeding ratio, DT yield fraction (mostly from T originating from D(d,p)T reactions of the majority DD fuel), and total fusion yield as a function of the DT core ρR_{DT}.

7. Conclusions

Success of experiments, theory and simulations on interaction of intense heavy ion beams with plasmas have led to significant scientific advances in transverse and longitudinal compression of heavy ion beams, to be applied to high energy density physics and fusion. The present and planned research should provide the physics knowledge base needed to optimize the design of future heavy ion accelerators as drivers for both high energy density physics and fusion. High efficiency direct-drive enabled by neutralized beam compression and focusing offers the possibility of using self-breeding T-lean targets and direct conversion for heavy ion fusion.

8. References

[1] P K Roy, S S Yu, S Eylon, E Henestroza, A Anders, E P Gilson, F M Bieniosek, W G Greenway, B G Logan, W L Waldron, D B Shuman, D L Vanecek, D R Welch, D V Rose, C Thoma, R C Davidson, P C Efthimion, I Kaganovich, A B Sefkow and W M Sharp 2005 *Nucl. Instr. Meth. Phys. Res*. **A544** 225

[2] C Thoma, D R Welch, S S Yu, E Henestroza, P K Roy, S Eylon and E P Gilson 2005 *Phys. of Plasmas* **12** 043102

[3] P K Roy, S S Yu, E Henestroza, A Anders, F M Bieniosek, J Coleman, S Eylon, W G Greenway, M Leitner, B G Logan, W L Waldron, D R Welch, C Thoma, A B Sefkow, E P Gilson, P C Efthimion, and R C Davidson 2005 *Phys. Rev. Lett.* **95,** 234801

[4] A B Sefkow, R C Davidson, P C Efthimion, E P Gilson, S S Yu, P K Roy, F M Bieniosek, J E Coleman, S Eylon, W G Greenway, E Henestroza, J W Kwan, D L Vanecek, W L Waldron and D R Welch 2006 *Phys. Rev. ST Accel. Beams* **9,** 052801

[5] P A Ni, J J Barnard, F M Bieniosek, D Fernengel, A Fertman, A A Golubev, D H Hoffmann, A Hug, M. Kulish, M Leitner, B G Logan, J Menzel, R M More, D N Nikolaev, P K Roy, B Yu. Sharkov, N A Tahir, V Ya. Ternovoi, V Turtikov, S Udrea, D Varentsov and H Wahl, 2007 *Proc. of 2007 Particle Accelerator Conf.* (IEEE, Piscataway, NJ), in press.
[6] D H H Hoffmann, A Blazevic, P Ni, O Rosmej, M Roth, N A Tahir, A Tauschwitz, S Udrea, D Varentsov, K Weyrich and Y Maron, 2005 *Laser Part. Beams* 23 47
[7] N A Tahir, et.al., 2005 *Nucl. Instr. Meth*. A544, 16-26.
[8] F Becker, A Hug, P Forck, M. Kulish, P Ni, S Udrea and D Varentsov, 2005 *Laser and Particle Beams,* Volume 24, Issue 04, pp 541-551.
[9] P. Ni, PhD thesis, Technical University of Darmstadt (2006), http://elib.tudarmstadt. de/diss/000720
[10] A W Molvik, M Kireeff Covo, R Cohen, J Coleman, W Sharp, J-L Vay, D Baca, F Bieniosek, A Friedman, C Leister, P K Roy, P Seidl, and K van den Bogert, *Proceedings of Ecloud07, Daegu, Korea, 9-13 April 2007.*
[11] A W Molvik, J-L. Vay, M Kireeff Covo, R Cohen, D Baca, F Bieniosek, A Friedman, C Leister, S M Lund, P Seidl, and W Sharp, 2007 *Phys. Plasmas* **14**, 056701.
[12] M Kireeff Covo, A Molvik, A Friedman, R Cohen, J-L Vay, F Bieniosek, D Baca, P A Seidl, G Logan,, and J L Vujic; submitted to *Nucl. Instr. and Meth*. **B**.
[13] R C Davidson, B G Logan, J J Barnard et al., 2006 *Journal de Physique France* **133**, 731
[14] ID Kaganovich, AB Sefkow, EA Startsev, RC Davidson and DR Welch, 2007 *Nucl Inst. and Meth.* A577, 93.
[15] J S Pennington, I D Kaganovich, A B Sefkow, E A Startsev and R C Davidson, *Proc. of the 2007 Particle Accelerator Conf.*, in press.
[16] E A Startsev and R C Davidson, 2006 *Physics of Plasmas* 13, 062108.
[17] E A Startsev and R C Davidson, 2007 *Nucl. Instr. Meth.* A577, 79.
[18] A B Sefkow and R C Davidson, 2006 *Phys. Rev. ST Accel. Beams* 9, 090101.
[19] R. C. Davidson, M. Dorf, I. D. Kaganovich, H. Qin, A. B. Sefkow and E A Startsev, D R Welch, D V Rose and S M Lund, 2007 *Nucl. Instr. Meth.* A577, 70.
[20] E A Startsev, R C Davidson and H Qin, 2007 *Physics of Plasmas* 14, 056705.
[21] H Qin, R C Davidson and E A Startsev, 2007 *Nucl. Instr. Meth.* A577, 86.
[22] H Qin, R C Davidson and E A Startsev, 2007 *Phys. Rev. ST Accel. Beams* 10, 064201.
[23] H Qin, R C Davidson and E A Startsev, *Proc. of the 2007 Particle Accelerator Conf.,* in press.
[24] M Dorf, R C Davidson and E A Startsev, 2006 *Phys. Rev. ST Accel. Beams* 9, 034202.
[25] I D Kaganovich, E A Startsev and R C Davidson, 2006 *New Journal of Physics* 8, 278.
[26] A Shnidman, I D Kaganovich, and R C Davidson, *Proc. 2007 Particle Accelerator Conf*, in press.
[27] S M Lund, T Kikuchi and R C Davidson, submitted to 2007 *Phys. Rev. ST Accel. Beams* 10.
[28] A B Sefkow, R C Davidson, I D Kaganovich , E P Gilson, P K Roy, S S Yu, P A Seidl, D R Welch, D V Rose and J J Barnard, 2007 *Nucl. Instr. Meth.* A577, 289.
[29] A B Sefkow and R C Davidson, submitted to 2007 *Phys. Rev. ST Accel. Beams* 10.
[30] A B Sefkow, R C Davidson, P C Efthimion, E P Gilson, I D Kaganovich, J E Coleman, P K Roy, P A Seidl , J J Barnard, and D R Welch, *Proc. 2007 Particle Accelerator Conf.,* in press.
[31] A B Sefkow, R C Davidson and E P Gilson, submitted to 2007 *Phys. Rev. ST Accel. Beams* 10.
[32] J-L Vay, 2007 Phys. Rev. Lett. **98**, 130405.
[33] A B Sefkow, *Current Density Compression of Intense Ion Beams, 2007 Ph.D. dissertation, Princeton University*.
[34] N Tahir and C Deutsch 1992 *Phys. Fluids.* B 4 3735 - 3746
[35] B G Logan, J J Barnard, K N LaFortune, E P Lee, R W Moir, L J Perkins, (June 2007), to be submitted to *Nuclear Fusion*.
[36] M Tabak 1996 *Nuclear Fusion* 36, No 2.
[37] S Atzeni, and C Ciampi, 1997 *Nuclear Fusion* 37, 1665.
[38] B G Logan, 1993 *Fusion Engineering and Design* **22**, 151.